Chapter 16
Characterisation of Catalysts and Adsorbents by Inverse Gas Chromatography

Eva Díaz and Salvador Ordóñez

Abstract Inverse Gas Chromatography (IGC), in contrast to analytical chromatography, consists on adsorption of a known solute on an adsorbent whose properties are to be determined. The shape and positions of the peaks supply information about the nature and reactivity of the solid surface. If different probe molecules are used (i.e. polar and apolar molecules, molecules with acid/base properties), it is possible to study the specificity of these interactions. Therefore, IGC can be used both as a tool for both characterizing the adsorption of a given compound on a given solid or for studying the nature (in terms of acid-base properties, polar or apolar interactions, etc.) of the active sites of a certain catalyst.

16.1 Introduction

Sorption measurements are a useful method in the characterization of solid materials. From these data, it is possible to obtain information about the capacity of adsorption, but also thermodynamic properties—enthalpies of adsorption, surface energy—as well as kinetic information, such as diffusion rates. Sorption measurements can be obtained either by static or dynamic methods. Static methods carried out the adsorption measurements under vacuum, after a pre-treatment at high temperature in order to clean the material surface. Dynamic methods use a flowing gas device. Inverse gas chromatography (IGC) is a dynamic method. In comparison to static adsorption systems, dynamic sorption techniques show shorter measurement time, and a wider range of experimental possibilities.

In contrast to analytical chromatography, the stationary phase is the sample under investigation, and the mobile phase acts as probe molecule. Thus, the roles of the

E. Díaz (✉) · S. Ordóñez
Department of Chemical Engineering and Environmental Technology, Faculty of Chemistry, University of Oviedo, C/ Julián Clavería s/n, 33006 Oviedo, Spain
e-mail: diazfeva@uniovi.es

A. Auroux (ed.), *Calorimetry and Thermal Methods in Catalysis*,
Springer Series in Materials Science 154, DOI: 10.1007/978-3-642-11954-5_16,

phases are inverted and hence, the name of "inverse" gas chromatography. This technique involves injecting a series of volatile probes and measuring their retention volumes. Retention volume is related to the interaction parameters between the probes and the solid and can be converted into a number of surface thermodynamic properties. Through an adequate choice of the probe molecules to be adsorbed, it is possible to obtain information about the surface structure and/or surface functionality of adsorbents. After the introduction of the technique and subsequent theoretical developments, the application of IGC in the materials sciences has developed fast [1]. IGC has been used for the characterization of polymers, copolymers, polymer bends, biopolymers, industrial fibers, wood and pulp fibers, composites, coatings, pigments, catalysts, glass beads, coal, chemicals, and steel tubing [2].

Inverse chromatography can be used in the gas phase as well as in the liquid phase. Although there is some interest in the research of the solid in liquid phase, a vast literature has done o gas phase (IGC), thus this chapter will be centred in IGC.

16.2 Experimental

IGC measurements can be carried out using a pulse or continuous technique. The pulse of probe molecule is introduced into the carrier gas stream. This pulse is transported by the carrier gas through the system to the column with the solid sample. On the stationary phase, adsorption and desorption occur and the result is a peak in the chromatogram. The ratio of adsorption/desorption is governed by the partition coefficient. At fixed conditions of temperature and flow rate, the time of retention of a compound is characteristic of the system. An alternative is the frontal technique. This is carried out by injection into the carrier gas stream of a continuous stream of the probe molecule. When the sample enters into the column, there is a distribution between phases, and the concentration profiles takes the shape of a plateau, preceded by a breakthrough curve. The shape of this curve is characteristic of each system [3]. The benefit of the frontal technique is that equilibrium can be always established due to its continuous nature while pulse chromatography requires the assumption of a fast equilibration of the probe molecule adsorption on the surface. Between both techniques, the main part of publications describes pulse experiences, since they are faster, easier to control and more accurate, especially if interactions between probe molecules and the adsorbent are weak.

The experimental set-up for the pulse chromatographic experiments consists of a column inside an oven, with an inlet of the carrier gas with the probe molecule, and the detector at the exit of the column. The pure carrier gas is introduced into the column (packed with the material under study). The injection of the sample takes place prior the oven of the chromatograph and it can be done by different methods [4]:

- by a syringe via the manual injector port of the chromatographic device, consisting of vapor or liquid;

- by a vapour headspace system, in this case a carrier gas is passed through a reservoir containing the prove molecule in its liquid form. The gas is saturated with the prove molecule and then flowing through the injection loop. Concentration can be controlled by the temperature in the reservoir and the loop volume. This saturated carrier gas is injected into another pure carrier gas stream.

Concerning the carrier gas, helium or nitrogen, the most important requirement is to ensure its purity and dryness, since some adsorption processes are highly sensitive to traces of impurities, in particular moisture. Add to the retention time of the probe molecule, it is necessary also to know the dead-time of the system—time that the probe molecule would require travelling along the column without any interaction. Obviously, this dead-time can not be measured using the probe molecule since interactions will be always present. Thus, another molecule, knows as tracer, with negligible interactions with both the adsorbents and the column walls is employed. Usual tracers molecules are methane, hydrogen, nitrogen, or even air. The retention time, as well as the area under the peak, is measured by flame ionisation (FID) or thermal conductivity (TCD) detector. The FID has the benefit of the sensitive, but it is limited to organic samples, while TCD is more versatile. Occasionally mass spectrometric detectors are also used. This is particularly interesting for experiments where two o more probe molecules are injected.

As far as columns are concerned, they are constructed from glass or metal tubes. Furthermore, in the case of metals, they are usually stainless steel column, with passivated inner walls to avoid interactions. In the literature, there is a wide variety about column lengths and diameters for different applications. The main criteria for selecting column dimensions are the following [4, 5]:

- Small column diameter, in order to keep gas-phase diffusion effects to minimum.
- Ratio between the column diameter and the particle diameter:

$$D_{in}/d_p > 10 \tag{16.1}$$

  This ratio between both diameters ensures minimization of the effect of channelling at the wall.
- Ratio between the column length and the particle diameter:

$$L/d_p > 50 \tag{16.2}$$

  This ratio minimizes the axial dispersion. The column length is not so crucial as the bed length of the packed stationary phase. Usually packed beds are supported on a porous filter or hold in place with glass wool plugs. For this reason, the column can be longer than the packing. To avoid additional peak broadening is recommended to pack the free place with inert material of the same particle size (glass), Fig. 16.1. The length of the packing depends on the uptake capacity of the sample and the amount of probe injected. It must be sure that the retention is strong enough (good separation between probe and tracer peak) to obtain reproducible and accurate results. This can be checked by repeating the column with different masses. If the

Fig. 16.1 Scheme of column packing and inert material disposition

measured parameters are independent of mass of the adsorbent, enough amount of packing is used.

- Particle size should be selected to minimize the effects of intraparticular diffusion.

Concerning the flow rate, it is supposed that the lower the flow rate the more likely the equilibrium of a system is reached. However, low flow rates mean longer experimental times and broader peaks, thus accuracy in the retention time determination is decreased. A chromatographic column can be considered as a sum of discrete but contiguous narrow layers, or plates. At each plate, equilibration of the solute between the mobile and stationary phase was assumed to take place. Movement of the solute down the column was then treated as a stepwise transfer of equilibrated mobile phase from one plate to the next. So, a chromatographic column is constituted by a number of steps, N, with a length, L. Efficiency studies of a chromatographic column have generally been carried out by determining H as a function of mobile-phase velocity u, according to the van Deemter equation (Eq. 16.3) [6]:

$$\mathrm{H} = \mathrm{A} + \frac{\mathrm{B}}{u} + \mathrm{C}u = \mathrm{A} + \frac{\mathrm{B}}{\mathrm{u}} + (\mathrm{C_S} + \mathrm{C_M})u \tag{16.3}$$

where H is the plate height in centimeters; u, the linear velocity of the mobile phase in centimeters per second; and the quantities A, B, and C are coefficients related to the phenomena of multiple flow paths, longitudinal diffusion, and mass transfer between phases, respectively. The C coefficient can be divided into two coefficients, one related to the stationary phase (C_s) and one related to the mobile phase (C_M). The van Deemter equation contains terms linearly and inversely proportional to, as well as independent of, the mobile phase velocity. Taking into account these considerations, it is recommended to repeat the experiment at different flow rates and determine the optimum (minimum H) via van Deemter equation, Fig. 16.2a.

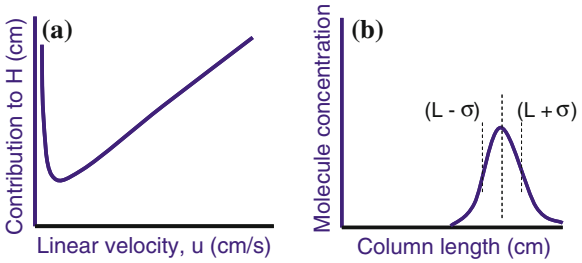

Fig. 16.2 **a** Plot of the plate height versus the mobile phase velocity; **b** Calculation of plate height

The plate height, H, is given by, Eq. (16.4):

$$H = \frac{\sigma^2}{L} \tag{16.4}$$

Thus, the plate height can be obtained from the length of column that contains a fraction of the probe molecule that lies between $L - \sigma$ and L (Fig. 16.2b). Because the area under a normal error curve bounded by σ is about 68 % of the total area, the plate height, as defined, contains approximately 34 % of the probe molecule.

Once the plate height is known, the number of plates of the column is obtained directly from the length of the chromatographic column ($N = L/H$).

Taking into consideration the aforementioned points related to both the column dimensions and packing and the gas flow rate, and working at very low concentrations of adsorbate, symmetric peaks are obtained for many materials. Under these conditions, the hypothesis of infinite dilution can be considered. Due to several both experimental conditions and instrumental problems, broadening of the peaks can be observed—avoiding the use of the Gaussian peak, explained later. Some of these causes are:

- Inadequate column dimensions, amount of stationary phase or gas flow rate, thus axial dispersion could be the responsible of the broadening.
- Large volume of adsorbate injections.
- Dead volumes in detector or injector.
- Imperfect column packing.

However, sometimes, even working at very low concentrations of the probe molecule and following the aforementioned recommendations, peaks with a large broadening are obtained. In these cases, it can be assumed that this asymmetry is not due to instrumental problems or experimental conditions. This effect is characteristic of the so-called "slow kinetic process" [7], Fig. 16.3, associated with markedly energetically heterogeneous surfaces containing preferential sites were desorption takes place in a slower way. Slow kinetic process depends on the concentration of the

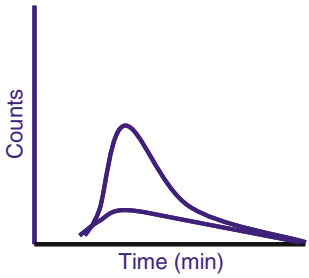

Fig. 16.3 Effect of slow kinetic process

solute, and is attenuated when the amount of adsorptive is decreased. Moreover, they correspond to non equilibrium situations, thus the gas flow rate have a significant effect on it.

16.3 Adsorption Isotherms

Adsorption isotherms of gases or vapors are the basis upon which the surface characteristics of adsorbents are defined. From this magnitude, specific surface area, porosity and other properties of the solid can be obtained. Even more, using adsorbates with diverse physical and chemical characteristics, it is possible to define the type of adsorbate-adsorbent interactions involved and the nature of the adsorption in the system tested. From the chromatographic peaks, the adsorption isotherms can be directly obtained. Figure 16.4 presents a general relation between the chromatographic peak and the adsorption isotherm shape. In the case of infinite dilution, a symmetrical (gaussian) peak is observed representing a linear Henry isotherm. At high concentration (finite dilution) tailing or leading will occur. In the case of a type I, II, or IV isotherm there is a tailing because adsorbent/adsorbate interactions are much stronger than adsorbate/adsorbate interactions.

Glückauf [8, 9] develop a method for obtaining the adsorption isotherms from chromatographic peaks in which a continuous stream of adsorbate is injected into the column until saturation, and the adsorbed material is then eluted by a pure carrier gas stream. The adsorption isotherm is calculated from the shape of the desorption curve. Gregg and Stock [10, 11] demonstrated that it was possible to obtained the adsorption isotherms from chromatographic data for all types of Brunauer isotherm. For this purpose, high concentrations of adsorbate are applied, but the effect of gradient pressure was neglected in most of the experimental work published before 1968 [12]. Taking into account these considerations, adsorption isotherms can be obtained either from the ideal GC, at conditions of infinite dilution, or by non-ideal and non-linear chromatography, at conditions of finite dilution. Ideal GC is described here, whereas finite chromatography isotherms determination can be found in the literature [3, 12].

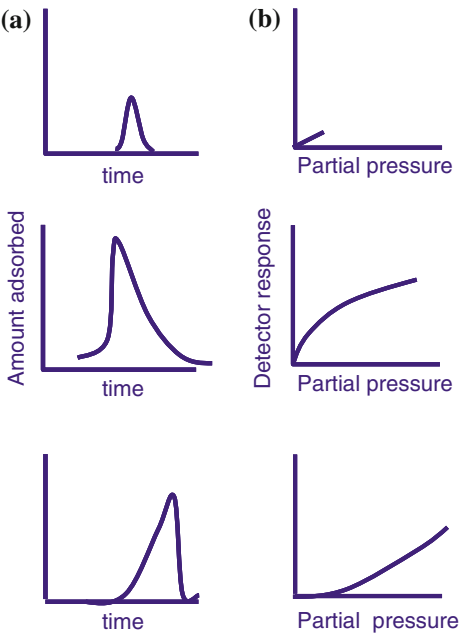

Fig. 16.4 Correlation of peak form **a** and adsorption isotherm **b** for finite and infinite dilution

At conditions in a chromatographic columns which approach the requirements of ideal IGC (minimum of van Deemter curve), the following hypothesis can be supposed:

- Flow through the column under isothermic and isobaric conditions
- Fast fluid-solid transfer
- Negligible intraparticular diffusion
- Axial transport due to convection
- No concentration or velocity gradients in radial direction
- Reversible adsorption and instantaneous equilibrium

In this case, diffusional and kinetical broadening of the chromatographic column is reduced, and any distortion of the chromatogram is due to the deviation of the adsorption isotherm from the Henry's law.

Therefore, it can be described the change in adsorbate concentration across an increment of the chromatographic column of length *dx* as:

$$-\mathrm{u_0 v}\left(\frac{\partial \mathrm{c}}{\partial \mathrm{x}}\right)_{\mathrm{t}} = \mathrm{v}\left(\frac{\partial \mathrm{c}}{\partial \mathrm{t}}\right)_{\mathrm{x}} + \mathrm{v_a}\left(\frac{\partial \mathrm{c_a}}{\partial \mathrm{t}}\right)_{\mathrm{x}} \tag{16.5}$$

where u_0 is the lineal gas velocity; v, the gas phase volume in the column; v_a, the volume of adsorbate retained on the adsorbent; c, the adsorbate concentration in gas phase; c_a, the adsorbate concentration on the adsorbent; t, the time since the injection, and x, the length from the beginning of the column and the dx. The first part of the

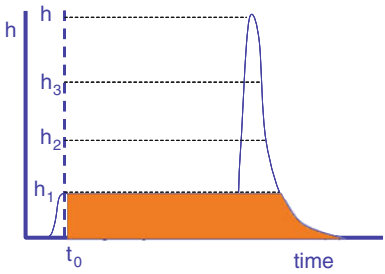

Fig. 16.5 Graphic integration of chromatogram and determination of the adsorption isotherm by the ECP method

mass balance corresponds to the mass of adsorbate accumulated, whereas the second part represents the rate of change of the amount of adsorbate in the layer dx.

By successive calculations [12], it is possible to determine the magnitude of adsorption, a, for an equilibrium concentration of adsorbate, c, in the mobile phase:

$$\mathrm{a} = \frac{1}{\mathrm{m}} \int_0^{\mathrm{c}} \mathrm{V_R d}c \tag{16.6}$$

where m is the mass of adsorbent in the column, and V_R, the retention volume.

The most common method of obtaining adsorption isotherms is the Elution of a Characteristic Point (ECP) [13], which consists of obtaining the isotherm from just one single injection. By introducing into Eq. (16.6) the magnitudes obtained from the chromatogram, the detector constant, k, and giving the detector deflections, h, the value of adsorption, a, is obtained:

$$a = \frac{m_a S_{ads}}{m S_{peak}} \tag{16.7}$$

where m_a is the mass of injected adsorbate; S_{ads}, is the area bounded by the height h between the tracer peak and the extender profile of the chromatogram (Fig. 16.5), and S_{peak}, the peak area.

The equilibrium concentration of adsorbate in the mobile phase can be expressed as:

$$c = \frac{m_a h}{F S_{peak}} \tag{16.8}$$

where F is the flow rate of the carrier gas. The equilibrium pressure is determined from the equation $\mathrm{p} = \mathrm{cRT}$. After substituting in Eq. (16.8), it is obtained the expression to calculate the equilibrium pressure:

$$p = \frac{m_a h R T}{F S_{peak}} \tag{16.9}$$

From a theoretical point of view, the method is accurate and a single elution profile allows the determination of a complete isotherm [14]. The applicability is restricted to very efficient columns allowing fast mass transfer, that it, columns possessing a high plate number. Low concentration measurements allow also to determine Henry constants, in this range the uptake is independent of the surface coverage. This regime is ideal also for the measurement of thermodynamic parameters since they can be obtained with the highest sensitivity. The span of the infinite dilution range depends on the probe molecules and the heterogeneity of the material. Especially for polar probe molecules adsorbing on very heterogeneous surface, non-symmetrical peaks are often observed even with the smallest injection size/concentration. This suggests that the values obtained under these conditions are not truly representing Henry conditions; however, they are still use for practical considerations.

16.4 Thermodynamic Parameters

16.4.1 Retention Volume

Application of IGC to study the properties of a solid is based on the assumption that the adsorbate equilibrium conditions are achieved between the mobile and stationary phases. Thus, chromatogram should be symmetric and the maximum of the peak must not depend on the amount of the injected adsorbate. Moreover, as the amount of adsorbate is very small, the concentration of the adsorbate in the gas phase is minimal and the adsorption process is conditioned by the real adsorbate-adsorbent interactions. Under these conditions, the retention volume—key parameter in IGC- of the solute depends on its partition between the stationary and mobile phase, and is an indication of the interaction strength between the solute molecule and the metal/adsorbent surface. The specific retention volume, V_g, in cm^3/g, is given as:

$$V_g = Fj\frac{(t_R - t_d)}{m}\left(\frac{p_0 - p_w}{p_0}\right)\left(\frac{T}{T_{meter}}\right) \tag{16.10}$$

where F is the uncorrected flow rate detected by a bubble flow meter; t_R is the retention time in min; t_d, the hold-up time or time of a tracer compound in pass through the column; p_0, the outlet column pressure; p_w, the vapor pressure of water at the flowmeter temperature; T, the column temperature; T_{meter}, the ambient temperature, and j, the James-Martin compressibility factor. This parameter represents the volume of dry gas to elute the adsorbate, corrected at 273 K and per gram of stationary phase. Add to V_g, it is also very employed the net retention volume, V_N, defined as the volume of dry gas to elute the adsorbate, corrected at 273 K.

In both cases, the James-Martin factor for the correction of gas compressibility under pressure difference between column inlet, p_i, and column outlet, p_0, is introduced:

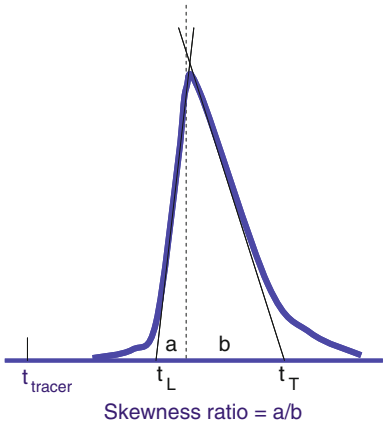

Fig. 16.6 Chromatogram presenting the Conder and Young method to obtain the skewness ratio (a/b) and retention time, t_R

$$j = \frac{3}{2}\left[\frac{(p_i/p_0)^2 - 1}{(p_i/p_0)^3 - 1}\right] \tag{16.11}$$

In the case of perfect symmetric peaks, the retention time can be determined directly from the peak maximum method, which is the simplest and most common. The peak maximum method is useful for determination of retention time if the skewness ratio is 0.7–1.3 [15]. The "skewness ratio" is defined as the ratio of tangent slope to the peak leading part and tangent slope to the peak tailing part whereas both tangents are drawn in the inflexion points. In such cases the skewness ratio is our of this interval, t_R is obtained from the first-order moment method or the Conder and Young method. Between these two methods, Conder and Young is recommended [16]:

$$t_R = (t_L + t_T)/2 \tag{16.12}$$

where t_L and t_T are the times at which the tangents drawn to the peak leading and tailing parts in their inflexion points intersect the zero line, Fig. 16.6.

The retention volume is related to the surface area and surface energy; that is, the higher the surface area and energy, the higher the retention time, and therefore, retention volume.

Moreover, the V_N and the slope of adsorption isotherm are related by Eq. (16.13) for small adsorbate injections, where conditions of "infinite dilution" are achieved:

$$V_N = K_S \cdot A = \frac{q}{c} \cdot A \tag{16.13}$$

where K_s is the inclination of the isotherm at infinite dilution, that is, the Henry's constant; A, the specific surface area of the adsorbent; q, concentration of the adsorbate in the stationary phase, and c, concentration of the adsorbate in the gas phase.

16.4.2 Free Energy of Adsorption

Thermodynamics information of the adsorption process at infinite dilution can be obtained from the retention volume. At infinite dilution, the standard free energy to transfer 1 mol of adsorbate from the gas phase to the surface at standard state, defined as the variation in the standard free energy of adsorption, ΔG^0_{ads} (J/mol), can be expressed as:

$$\Delta G^0_{ads} = -RT \ln \left[\frac{P V_g}{\pi_0 A} \right] \tag{16.14}$$

or its equivalent form:

$$\Delta G^0_{ads} = -RT \ln V_g + C \tag{16.15}$$

where P is the gas phase pressure, A is the specific surface area of the adsorbent, and π_0 is the spreading pressure of the adsorbed gas. Two different standard states can be considered: in the De Boer state, the spreading pressure has a value of 338 μN/m [17] at $p_0 = 1.01\,\text{kN/m}^2$, whereas in the Kemball and Rideal state, at $p_0 = 1.01\,\text{kN/m}^2$, the spreading pressure is 0.0608 μN/m [18]. The parameter, C, is a constant related to the standard reference states:

$$C = -RT \ln \left(\frac{A\pi}{P} \right) \tag{16.16}$$

16.4.3 Enthalpy and Entropy of Adsorption

When zero coverage (infinite dilution) conditions are fulfilled the standard differential heat of adsorption, q_0, is numerically equal to the opposite of the enthalpy of the process. This value can be obtained from the variation of ΔG^0_{ads} with temperature. For an equilibrium process this variation is given by Gibbs-Helmholtz equation:

$$\left[\frac{\partial \left(-\Delta G^0_{ads}/T \right)}{\partial (1/T)} \right]_P = \left[R \frac{\partial \left(\ln V_N \right)}{\partial \left(1/T \right)} \right]_P = q^0 \tag{16.17}$$

In the Fig. 16.7 is illustrated the dependence of $-\Delta G^0_{ads}/T$ as a function of $1/T$ for conventional carbon fibers and carbon fibers oxidized by electrochemical procedure. In the figure is illustrated the dependence of *n*-heptane. This behaviour, typical of hydrocarbons, implies that ΔH^0_{ads} is constant within the temperature range of characterisation. At this point, it is important to remark that comparison of differential heats of adsorption with the heats of liquefaction is recommended, in order to ensure the nature of the interaction. In the cases where the adsorbate-adsorbent interactions are stronger than adsorbate-adsorbate interactions, ΔH^0_{ads} is higher than the liquefaction heat.

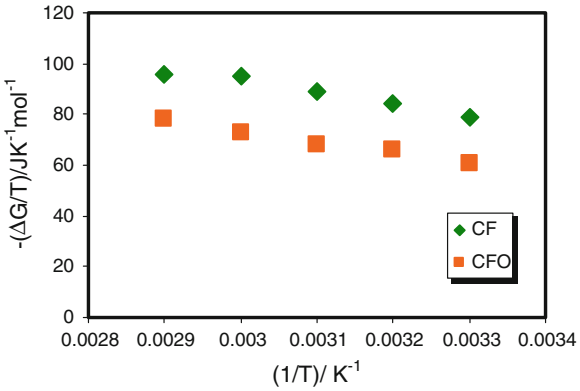

Fig. 16.7 Variation of $(-\Delta G^0_{ads}/T)$ with $(1/T)$ for the adsorption of *n*-heptane on carbon fibers (adapted from Ref. [19])

From the adsorption standard free energies and standard enthalpies, adsorption entropies can be calculated from:

$$\Delta S^0_{ads} = -\frac{\left(q^0 + \Delta G^0_{ads}\right)}{T} = \frac{\Delta H^0_{ads} - \Delta G^0_{ads}}{T} \tag{16.18}$$

In agreement with the linearity in the $-\Delta G^0_{ads}$/T versus $1/T$, the adsorption entropies are independent of the temperature.

Figure 16.8 shows the existence of so-called "thermodynamic compensation effect", i.e. a linear dependence of ΔH^0_{ads} on ΔS^0_{ads}. Thermodynamic compensation effect between the adsorption enthalpy and entropy was observed in different studies for *n*-alkanes. It indicates that the stronger adsorption of longer *n*-alkanes is accompanied by a higher loss of mobility of the molecules (it means higher interaction between the molecule and the surface). This type of plot is used currently to highlight the differences in adsorbate-adsorbent interactions. A good fit of the compensation effect data to a straight line indicates the non-specific nature of the adsorbate-adsorbent interactions.

In the case of Fig. 16.8, three straight lines are depicted, one corresponding to the data of HSAG-100 and HSAG-300, and two more fitting the CNTs and CNFs points. Although the line of CNFs is clearly shifted with respect to graphites, the slope of both lines is virtually the same and different from that of CNTs. Since the adsorbate type is the same for both sets of data (*n*-alkanes), the difference in slopes can be attributed to the existence of two different non-specific surfaces, one of the CNFs and graphites and the other represented by the CNTs [19]. Likewise, the shift between graphites and CNFs could be understood since HSAGs contain a large amount of structural defects, so the interactions could be modified. It is also evident the higher values of entropy for the nanotubes in comparison with the other materials, due to high entropy of adsorbate located inside the tubes [21].

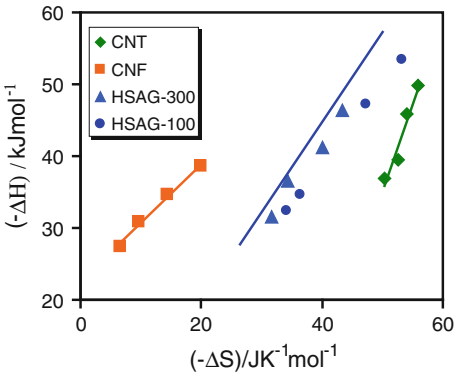

Fig. 16.8 Thermodynamic compensation effect of *n*-alkanes on carbon nanotubes (CNT), carbon nanofibers (CNF) and high-surface-area-graphites (HSAG) (adapted from Ref. [20])

16.4.4 Work of Adhesion: Dispersive and Specific Contribution

In the absence of chemisorption and interdiffusion, the work of adhesion is the sum of the different intermolecular forces involved and can be related to the surface free energies, where a is the compound and the superscripts *D* and *S* denote dispersive and specific interactions:

$$\mathrm{W_a} = \mathrm{W_a^D} + \mathrm{W_a^S} \tag{16.19}$$

Generally, the work of adhesion is coupled to ΔG^0_{ads} according to:

$$\Delta \mathrm{G_{ads}} = -\mathrm{NaW_a} \tag{16.20}$$

where N is the Avogadro's number and a is the surface area of a single probe molecule.

For two materials interacting only via London dispersive forces across their interface, Fowkes [22–24] suggested that the work of adhesion, W_a, could be described as the geometric mean approach, where γ_L^D and γ_S^D are the dispersive component of the surface energy of the liquid (the probe) and the solid, respectively:

$$\mathrm{W_a} = \mathrm{W_a^D} = 2\sqrt{\gamma_\mathrm{L}^\mathrm{D}\gamma_\mathrm{S}^\mathrm{D}} \tag{16.21}$$

For probes interacting with the solid of interest via dispersive forces, a combination of Eqs. (16.15, 16.20, 16.21) will lead to:

$$\mathrm{RT\ln V_N} = 2\mathrm{N}\cdot\mathrm{a}\cdot\sqrt{\gamma_\mathrm{L}^\mathrm{D}\gamma_\mathrm{S}^\mathrm{D}} + \mathrm{K} \tag{16.22}$$

Thus, according to this approach, developed by Schultz et al. [25], by measuring the net retention volume for various *n*-alkane probes and plotting $RTlnV_N$ versus $a(\gamma_L^D)^{0.5}$, the dispersive component of the surface free energy can be determined

from the slope of a linear fit. The surface free energy is the energy required to form (or increase the surface by) a unit surface under reversible conditions and is the analogue to the surface tension of a liquid. From the practical point of view, the higher the surface energy, the more reactive the surface.

In the Schultz expression, it is necessary the molecular area. It can be determined from the liquid density, ρ, assuming a spherical molecular shape in a hexagonal close-packing configuration:

$$\mathrm{a} = 1.09 \cdot 10^{14} \left(\frac{\mathrm{M}}{\rho\, \mathrm{N}} \right)^{2/3} \tag{16.23}$$

where M is the molecular weight of the probe molecule.

However, some authors have stressed the difficulties associated with the determination of the molecular area, especially for non-spherical molecules such as straight alkanes. To avoid the problems derived from the molecular area, Dorris and Gray [26] considered the adsorption characteristics of single methylene groups in the n-alkane probes. By defining the increment in free energy of adsorption per – CH_2- unit:

$$\Delta \mathrm{G}_{\mathrm{CH_2}} = -\mathrm{RT} \ln \frac{\mathrm{V_{N(n)}}}{\mathrm{V_{N(n+1)}}} \tag{16.24}$$

where V_N and $V_{N+1}$are the retention volumes of n-alkanes with (n) and $(n + 1)$ carbon atoms, respectively. In this way, γ_S^D can be determined from:

$$\gamma_{\mathrm{S}}^{\mathrm{D}} = \frac{1}{4} \frac{\Delta \mathrm{G}_{\mathrm{CH_2}}^2}{\gamma_{\mathrm{CH_2}} \mathrm{N}^2 \mathrm{a}_{\mathrm{CH_2}}^2} \tag{16.25}$$

The benefit of this approach is the fact that despite the use of various n-alkanes probes, only methylene area, a_{CH_2}, and surface tension, γ_{CH_2}, have to be known. The CH_2 area is takes as $0.06\,\mathrm{nm}^2$, based on C–C length of 0.127 nm and an average distance of 0.47 nm for two CH_2 [26]. Jacob and Berg [27] have found extraordinary an excellent agreement between n-alkane molecular areas as determined from the fitting of experimental adsorption isotherms to the BET model and as obtained by simply assuming the area of $0.06\,\mathrm{nm}^2$ for each methylene group. The parameter $\gamma_{CH_2}$is estimated from the surface tension of a linear polyethylene melt as function of temperature:

$$\gamma_{\mathrm{CH_2}}(\mathrm{mJ/m^2}) = 35.6 + 0.058\left(20 - \mathrm{T}(^{\circ}\mathrm{C})\right) \tag{16.26}$$

The validity of this approach has established on the basis that IGC and wettability measurements lead to approximately the same γ_S^D value for poly(ethylene terephthalate) [28]. Furthermore, Dorris and Gray stated that the molecular area could be an adjustable parameter.

Once the dispersive interactions of a surface have been investigated, specific interactions can be studied by injecting polar probes. For these probes, W_a^S is usually

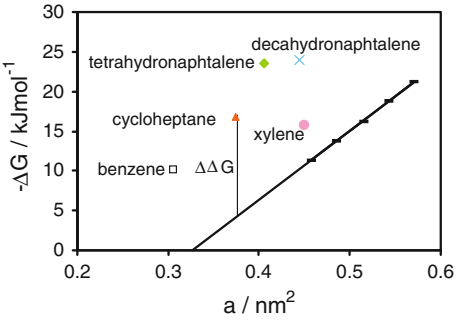

Fig. 16.9 Determination of the specific interaction parameter, I^{sp}, for polar probes on Al_2O_3 at 250 °C (adapted from Ref. [32])

larger than zero, which leads to increased net retention volumes as compared to *n*-alkanes. The adsorption of these molecules on the stationary phase is influenced, not only be dispersive interactions, but also by additional specific contributions. These specific contributions include dipole-dipole and acid-base interactions, the latter involving much higher energies than the former ones [35]. In fact, it is usually assumed that the specific contribution of the adsorption of polar probes are actually acid-base interaction only. In this way, Fowkes, by analogy with the dispersive work of adhesion, described the "extended Fowkes equation":

$$W_a^S = 2\sqrt{\gamma_L^S \gamma_S^S} \tag{16.27}$$

However, this expression can not predict accurately the magnitude of the non dispersive interactions, since it is wrong the assumption that the contribution to the work of adhesion of two polar compounds could be represented by the geometric mean value of their polar properties.

In order to quantify this specific contribution, several attempts were made. One is relate the specific component of the surface free energy to the parameter of specific interaction of polar solutes (I^{sp}). This parameter involves the surface properties in terms of potential and acid-base interactions and may be determined from the difference of free energy of adsorption, ($\Delta\Delta G$), between a polar solute and the real or hypothetical *n*-alkane with the same surface area, *a*, (Fig. 16.9):

$$I^{sp} = \frac{\Delta\,(\Delta G)}{Na} = \frac{\Delta G_{ads}^S}{Na} \tag{16.28}$$

Add to the surface area as parameter of comparison, the boiling point or the vapor pressure could also be used [29–31]. This treatment is essentially empirical, but it allows to compare the specific interaction between the surface and the solute molecules, based on a unified scale.

Donnet and coworkers [33, 34] obtained useless results with the above method when analyzing material with relative high dispersive component of the surface energy ($\gamma_S^D > 100\,mJ/m^2$), such as carbon nanofibers or graphite powders. For

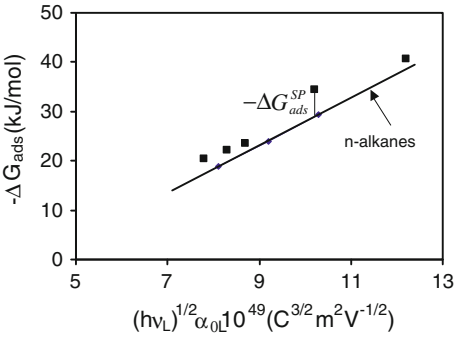

Fig. 16.10 Graphical description of the method followed to obtain the specific contribution of the adsorption free energy measured for different polar probes (adapted from Ref. [20])

these materials lower $(-\Delta G^0_{ads})$ values were found for the polar probes compared to reference *n*-alkanes. This problem can be encountered by plotting the free energy of adsorption as function of the molecular polarizability of the different polar adsorbates (Fig. 16.10):

$$-\Delta G^0_{ads} = \left(-\Delta G^D_0\right) + \left(-\Delta G^S_0\right)$$
$$= k_c\,(h\,\upsilon)^{1/2}\,\alpha_{0,s}\,(h\,\upsilon)^{1/2}\,\alpha_0 + \left(-\Delta G^S_0\right) \qquad (16.29)$$

where k_c, is the constant of the chromatographic process; h, the Planck constant (Js); υ, characteristic vibration frequency of the electron (s^{-1}); α_0, polarizability deformation (cm^2V^{-1}).

Since the free energy of ad Specific interactions $(-\Delta G^S_{ads})$ are determined from differences between $(-\Delta G^0_{ads})$ values of the polar probes and the reference line composed with data obtained from the elution of *n*-alkanes. In this way, $(-\Delta H^S_{ads})$ can be calculated from the variation of $(-\Delta G^S_{ads})$ versus $(1/T)$, as stated in Eq. (16.17). Therefore, the standard enthalpy of adsorption of polar probes is divided into two contributions, dispersive and specific:

$$\Delta H^0_{ads} = \Delta H^D_{ads} + \Delta H^S_{ads} \qquad (16.30)$$

The ability of the polar molecules to donate or accept electrons has been parameterized by means of the donor (DN) and acceptor (AN) number [35]. These parameters describe the basic and acidic nature, respectively. The DN values (kcal/mol) represent the enthalpy of formation for the adduct produced when the base in question reacts with the reference Lewis acid $SbCl_5$ in the 1,2-dichloromethane, as solvent. However, for the characterization of acids, no similar reference system was found. AN value (dimensionless) measuring the induced shift in the ^{31}P NMR spectra of the base Et_3PO_4 when this compound was dissolved in the acid under investigation. Riddle and Fowkes [36] corrected the AN scale to the enthalpy of reaction of Et_3PO_4 with $SbCl_5$. This new parameter, AN*, presents the same units as DN.

Thus, the measured $(-\Delta H^S_{ads})$ can be correlated to the acid and base indices AN* and DN of the solute probes [35], obtaining information about the surface acidity-basicity:

$$-\Delta H^S_{ads} = K_a \cdot DN + K_b \cdot AN^* \tag{16.31}$$

where K_a and K_b are indices reflecting the acidity (electron acceptor) and basicity (electron donor) of the solid surface. According to Eq. (16.31), a plot of versus (DN/AN*) should yield a straight line from which K_a can be obtained from the slope and K_b from the intercept. This equation is of empirical nature; other relationships have been also proposed in the literature [37].

16.4.5 Surface Heterogeneity

There is an important point that must be taken into account in the IGC determined parameters: for heterogeneous high energy surfaces, molecules will preferentially adsorb on the highest energy sites [38]. The distribution of energetic sites is usually called as surface heterogeneity. There exist two types of heterogeneity: structural and energetic. A typical example of a structural heterogeneity is a wide pore size distribution, where the geometrical effects determine the adsorption of the probe molecules. Energetic heterogeneity occurs with a wide distribution of various surface sites of different energetic levels. The energy heterogeneity can be described either by the adsorption energy distribution or the adsorption potential distribution.

For the determination of the adsorption energy distribution, $F(\varepsilon)$, from Eq. (16.32), and assumption on the shape of the local isotherms has to be made and usually complex numerical analysis is required [39, 40]:

$$\theta_t(p, T) = \int_{\varepsilon\,\min}^{\varepsilon\,\max} \theta_{1t}(\varepsilon, p, T) \cdot F(\varepsilon) \cdot d\varepsilon \tag{16.32}$$

where ε_{min} and ε_{max} indicate the range in potential energy of adsorption, and θ_t refers to the local adsorption isotherm.

Concerning the adsorption potential distribution, it can be obtained easily form the adsorption isotherm. Furthermore, is less affected by experimental noise and produce reliable results. Once the adsorption isotherm is derived from IGC, the adsorption potential, AP, is calculated according to:

$$AP = RT \ln\left(\frac{p_s}{p}\right) \tag{16.33}$$

where p is the partial pressure, and p_s, the saturation pressure.

The distribution parameter, ϕ, represents the first derivation of the adsorbed amount of molecules, n, with the adsorption potential:

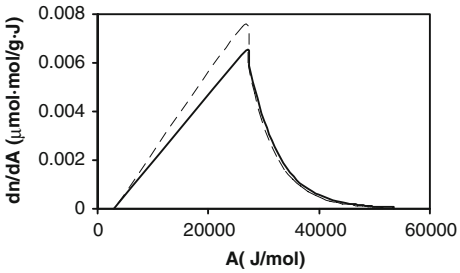

Fig. 16.11 Heterogeneity profiles of CNF (—) and CNF-oxi (--) at 250 °C for benzene (adapted from Ref. [41])

$$\phi = -\frac{\mathrm{d}n}{\mathrm{d}AP} \tag{16.34}$$

Figure 16.11 shows, as example, the adsorption potential distribution of benzene over two carbon nanofibers, a parent and an oxidized one. It can be seen that there is a good coincidence of the profiles; therefore, the adsorbates interact with the same energy sites. It means that the treatment of the nanofiber does not create new adsorption sites, just varying slightly the adsorption capacities (area under the curve).

16.5 Applications and Comparison to Other Techniques

Adsorption techniques have been widely applied both to know the adsorption capacity of the adsorbents and to obtain thermodynamic parameter for increasing the knowledge of the surface of the material. Static methods are, probably, the most used for these purposes, since they are considered the most accurate. Thus, comparison of the adsorption parameters obtained by other techniques with static methods is a usual way to ensure the reliability of a technique. Thielmann and Baumgarten [42] investigated the adsorption properties of four aluminas with different microporosities by both IGC and a static method. Sorption measurements obtained form IGC gave similar results whereas the static experiments showed differences until 37 %. This difference can be explained by a different micropore structure of the aluminas. This is so because one of the hypotheses assumed for obtaining adsorption data from the IGC eluted peak is to consider instantaneous adsorption equilibrium. In the case of microporous materials, transport of the solutes through the porous structure could delay the equilibrium, becoming more difficult to satisfy this hypothesis. Thus, the application of the IGC to microporous materials has been discouraged in the literature for microporous materials [4]. With the same aim of comparison between IGC and static techniques, different ion-exchanged zeolites (microporous materials) have been studied by gas calorimetry coupled to a volumetric line and IGC [43]. *n*-Hexane was used as adsorbate and isotherms of adsorption as well as the isosteric heats of adsorption and enthalpies of adsorption obtained, respectively, by the earlier mentioned methods were determined. The comparison between the volumetric adsorption

isotherms of *n*-hexane at 250 °C obtained both by IGC and calorimetry reveals that, at low pressures (when both techniques are applicable), the results obtained by both techniques are very similar. Moreover, the strength of adsorption is also quantify by the heat of adsorption (IGC) and the isosteric heat (calorimetry), obtaining deviations among them in the range of 4–20 %, depending on the material. Thus, at very low partial pressures, IGC could be a reliable technique even for microporous materials.

The wettability of powders is a valuable parameter in different fields such as the pharmacy [44], the ceramic [45], polymers [46] and nanomaterials [47]. Contact angle measurements are the most used in order to obtain information about the surface, however, IGC, by the dispersive component of the surface free energy could also offer a sensitive approach to surface characterization. In this way, comparison of the surface components using *n*-alkanes over theophylline and caffeine showed a good agreement [44]. It is important to mention that the method of calculating the γ_S^D value is applied to solid surfaces, flat at the molecular scales, presenting no chemical, structural or energetic heterogeneities. Thus, application of the method to other materials could give larger discordances. In this way, in a study of activated carbons characterization by IGC, Herry et al. [48] have obtained values of γ_S^D 10 times higher than the ones obtained previously by capillary wetting. This difference was attributed to the increase in the interaction potential in micropores. The discrepancy in the values obtained by the two techniques could be explained by assuming that the treatment of the column, prior to the IGC experiments, leads to carbon surfaces free from adsorbed species and other possible contaminants. Besides that, the contribution of high-energy sites will be significantly outweighed in IGC measurements under infinite dilution conditions. In fact, contact angle measurements are known to provide an average of the surface energy [49]. It is important to remark that in these situations, the ΔG_{CH_2} is more reliable, since it keeps a precise physical meaning [50].

Inverse gas chromatography parameters can also be applied in the field of catalysis. In this way, as example, parent NaX and CaA zeolites, as well as transition metal (Co^{2+}, Mn^{2+}, Fe^{3+})-exchanged zeolites, were evaluated for the catalytic oxidation of *n*-hexane. It was observed [51, 52], that although there was linear correlation between the acidity and the adsorption enthalpy of the *n*-hexane, there was no relationship between the acidity and the activity for *n*-hexane oxidation. However, if a reactivity parameter (such as T_{50}, temperature at which 50 % of conversion is attained) is plotted versus the adsorption heat, a so-called Volcano plot is obtained (Fig. 16.12), an optimum value of $(-\Delta H_{ads}^0)$ being observed, higher and lower values yielding to worst catalytic performance.

IGC was also use to elucidate the nature of the interaction of both reactives and products with the surface of heterogeneous catalysts in order to obtain information for understanding the mechanism of the reaction. Xie et al. [31] proposed a mechanism for the partial oxidation of propylene to acrylic acid based on the adsorption parameters of reactive and products on styrene divinylbenzene copolymer (SDB) and Pd supported on SDB. Likewise, Díaz et al. [53] studied the performance of Fe-ZSM-5 catalysts for benzylation of benzene with benzyl chloride in terms of their chemical and adsorption properties.

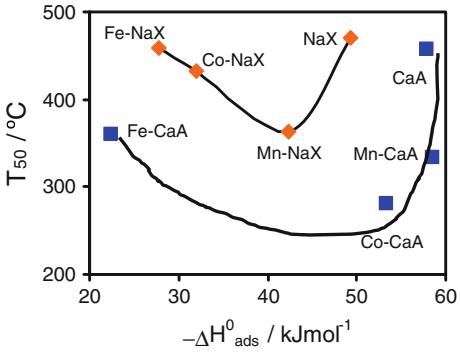

Fig. 16.12 Influence of the adsorption enthalpy of *n*-hexane of metal transition-exchanged zeolites on the T_{50} parameter (adapted from Ref. [52])

Finally, a mention to the reverse-flow (RF) GC technique, which is a variation of IGC where the probe molecule is injected at a middle point of the column containing the adsorbent as stationary phase, and the direction of carrier gas flow is reversed from time to time. This creates extra chromatographic peaks on the continuous signal. This technique allows to measured different physicochemical quantities, including rate constant of surface and gaseous reactions, and experimental isotherms [54, 55].

References

1. A.V. Kiselev, Adsorbents in gas chromatography, in *Advances in Chromatography*, ed. by J.C. Giddings, R.A. Keller (Marcel Dekker, New York, 1967)
2. A. Voelkel, Inverse gas-chromatography—characterization of polymers, fibers, modified silicas, and surfactants. Crit. Rev. Anal. Chem. **22**, 411–439 (1991). doi:10.1080/10408349108051641
3. V.R. Choudhary, L.K. Doraiswamy, Applications of gas chromatography in catalysis. Ind. Eng. Chem. Prod. Res. Develop. **10**, 218–237 (1971). doi:10.1021/i360039a002
4. F. Thielmann, Introduction into the characterisation of porous materials by inverse gas chromatography. J. Chromatogr. A **1037**, 115–123 (2004). doi:10.1016/j.chroma.2004.03.060
5. R.E. Hayes, S.T. Kolaczkowski, *Introduction to Catalytic Combustion* (Gordon and Breach Science Publisher, Amsterdam, 1997)
6. J. van Deemter, F.J. Zuiderweg, A. Klinkerberg, Longitudinal diffusion and resistance to mass transfer as causes of nonideality in chromatography. Chem. Eng. Sci. **5**, 271–289 (1956). doi:10.1016/0009-2509(56)80003-1
7. M. Montes-Morán, J.I. Paredes, A. Martínez-Alonso, J.M.D. Tascón, Adsorption of n-alkanes on plasma-oxidized high-strength carbon fibers. J. Colloid Interface Sci. **247**, 290–302 (2002). doi:10.1006/jcis.2001.8134
8. E. Glückauf, Adsorption isotherms from chromatographic measurements. Nature **156**, 748 (1945). doi:10.1038/156748c0
9. E. Glückauf, Theory of chromatography. Part II. Chromatograms of a single solute. J. Chem. Soc. 1302–1308 (1947). doi:10.1039/JR9470001302
10. S.J. Gregg, R. Stock, *Gas Chromatography* (Desty D.H, London, 1958)
11. S.J. Gregg, *The Surface Chemistry of Solids*, 2nd edn. (Chapman and Hall, London, 1961)
12. T. Paryjczak, *Gas Chromatography in Adsorption and Catalysis* (J. Wiley & Sons, New York, 1987)

13. E. Cremer, H. Huber, in *Gas Chromatogr: Instr Soc Amer Symp*, vol. 3, ed. by N. Brenner, et al. (Academic Press, New York, 1962), p. 169
14. A. Seidel-Morgenstern, Experimental determination of single solute and competitive adsorption isotherms. J. Chromatogr. A **1037**, 255–272 (2004). doi:10.1016/j.chroma.2003.11.108
15. J.R. Conder, S. McHale, M.A. Jones, Evaluation of methods of measuring gas-solid chromatographic retention on skewed peaks. Anal. Chem. **58**, 2663–2668 (1986). doi:10.1021/ac00126a019
16. B. Charmas, R. Leboda, Effect of surface heterogeneity on adsorption on solid surfaces: application of inverse gas chromatography in the studies of energetic heterogeneity of adsorbents. J. Chromatogr. A **886**, 133–152 (2000). doi:10.1016/S0021-9673(00)00432-5
17. J.H. De Boer, *The Dynamical Character of Adsorption* (Clarendon Press, Oxford, 1953)
18. C. Kemball, E.K. Rideal, The adsorption of vapours on mercury. I. Non-polar substances. Proc. R. Soc. A **187**, 53–73 (1946). doi:10.1098/rspa.1946.0065
19. M.A. Montes-Morán, A. Martínez-Alonso, J.M.D. Tascón, Effect of sizing on the surface properties of carbon fibres. J. Mater. Chem. **12**, 3843–3850 (2002). doi:10.1039/B202902B
20. E. Díaz, S. Ordóñez, A. Vega, Adsorption of volatile organic compounds onto carbon nanotubes, carbon nanofibers, and high-surface-area graphites. J. Colloid Interface Sci. **305**, 7–16 (2007). doi:10.1016/j.jcis.2006.09.036
21. S.Y. Bhide, S. Yashonath, Structure and dynamics of benzene in one-dimensional channels. J. Phys. Chem. B **104**, 11977–11986 (2000). doi:10.1021/jp002626h
22. F.M. Fowkes, Attractive forces at interface. Ind. Eng. Chem. **56**, 40–52 (1964). doi:10.1021/ie50660a008
23. F.M. Fowkes, Donor-acceptor interactions at interfaces. J. Adhesion **4**, 155–159 (1972). doi:10.1080/00218467208072219
24. F.M. Fowkes, M.A. Mostafa, Acid-base interactions in polymer adsorption. Ind. Eng. Chem. Prod. Res. Dev. **17**, 3–7 (1978). doi:10.1021/i360065a002
25. J. Schultz, L. Lavielle, C. Martin, The role of interface in carbon fiber-epoxy composites. J. Adhesion **23**, 45–60 (1987). doi:10.1080/00218468708080469
26. G.M. Dorris, D.G. Gray, Adsorption of n-alkanes at zero surface coverage on cellulose paper and wood fibers. J. Colloid Interface Sci. **77**, 353–362 (1980). doi:10.1016/0021-9797(80)90304-5
27. P.N. Jacob, J.C. Berg, Acid-base surface energy characterization of microcrystalline cellulose and two wood pulp fiber types using inverse gas chromatography. Langmuir **10**, 3086–3093 (1994). doi:10.1021/la00021a036
28. A. Pizzi, K.L. Mittal, *Handbook of Adhesive Technology* (Marcel Dekker, New York, 2003)
29. U. Panzer, H.P. Schreiber, On the evaluation of surface interactions by inverse gas chromatography. Macromolecules **25**, 3633–3637 (1992). doi:10.1021/ma00040a005
30. A. van Asten, N. van Veenendaal, S. Koster, Surface characterization of industrial fibers with inverse gas chromatography. J. Chromatogr. A **888**, 175–196 (2000). doi:10.1016/S0021-9673(00)00487-8
31. J. Xie, Q. Zhang, K.T. Chiang, An IGC study of Pd/SDB catalysts for partial oxidation of propylene to acrylic acid. J. Catal. **191**, 86–92 (2000). doi:10.1006/jcat.1999.2796
32. E. Díaz, S. Ordóñez, A. Vega, J. Coca, Adsorption properties of a Pd/γ-Al_2O_3 catalyst using inverse gas chromatography. Micropor. Mesopor. Mater. **70**, 109–118 (2004). doi:10.1016/j.micromeso.2004.03.005
33. S. Dong, M. Breadle, J.B. Donnet, Study of solid-surface polarity by inverse gas-chromatography at infinite dilution. Chromatographia **28**, 469–472 (1989). doi:10.1007/BF02261062
34. J.B. Donnet, S.J. Park, H. Balard, Evaluation of specific interactions of solid-surfaces by inverse gas-chromatography—a new approach based on polarizability of the probes. Chromatographia **31**, 434–440 (1991). doi:10.1007/BF02262385
35. V. Gutmann, *The Donor-Acceptor Approach to Molecular Interactions* (Plenum Press, New Cork, 1979)

36. F.L. Riddle, F.M. Fowkes, Spectral shifts in acid-base chemistry. 1. van der Waals contributions to acceptor numbers. J. Am. Chem. Soc. **112**, 3258–3264 (1990). doi:10.1021/ja00165a001
37. T. Hamieh, M. Nardin, M. Rageui-Lescourt, H. Haidara, J. Schultz, Study of acid-base interactions between some metallic oxides and model organic molecules. Colloids Surf. A **125**, 155–161 (1997). doi:10.1016/S0927-7757(96)03855-1
38. H. Ishida, *Characterization of Composite Materials* (Butterworth-Heinemann, London, 1994)
39. M. Pyda, G. Guiochon, Surface properties of silica-based adsorbents measured by inverse gas-solid chromatography at finite concentration. Langmuir **13**, 1020–1025 (1997). doi:10.1021/la950541f
40. H. Balard, A. Saada, E. Papirer, B. Siffert, Energetic surface heterogeneity of illites and kaolinites. Langmuir **13**, 1256–1259 (1997). doi:10.1021/la9515276
41. M.R. Cuervo, E. Asedegbega-Nieto, E. Díaz, A. Vega, S. Ordóñez, E. Castillejos-López, I. Rodríguez-Ramos, Effect of carbon nanofiber functionalization on the adsorption properties of volatile organic compounds. J. Chromatogr. A **1188**, 264–273 (2008). doi:10.1016/j.chroma.2008.02.061
42. F. Thielmann, E. Baumgarten, Characterization of microporous aluminas by inverse gas chromatography. J. Colloid Interface Sci. **229**, 418–422 (2000). doi:10.1006/jcis.2000.6958
43. E. Díaz, S. Ordóñez, A. Auroux, Comparative study on the gas-phase adsorption of hexane over zeolites by calorimetry and inverse gas chromatography. J. Chromatogr. A **1095**, 131–137 (2005). doi:10.1016/j.chroma.2005.07.117
44. J.W. Dove, G. Buckton, C. Doherty, A comparison of two contact angle measurement methods and inverse gas chromatography to assess the surface energies of theophylline and caffeine. Int. J. Pharm. **138**, 199–206 (1996). doi:10.1016/0378-5173(96)04535-8
45. C.-W. Won, B. Siffert, Preparation by sol-gel method of SiO_2 and mullite ($3Al_2O_3$, $2SiO_2$) powders and study of their surface characteristics by inverse gas chromatography and zetametry. Colloids Surf. A **131**, 161–172 (1998). doi:10.1016/S0927-7757(97)00149-0
46. R.A. Bailey, K.C. Persaud, Application of inverse gas chromatography to characterisation of a polypyrrole surface. Anal. Chim. Acta **363**, 147–156 (1998). doi:10.1016/S0003-2670(98)00084-1
47. K. Batko, A. Voelkel, Inverse gas chromatography as a tool for investigation of nanomaterials. J. Colloid Interface Sci. **315**, 768–771 (2007). doi:10.1016/j.jcis.2007.07.028
48. C. Herry, M. Baudu, D. Raveau, Estimation of the influence of structural elements of activated carbons on the energetic components of adsorption. Carbon **39**, 1879–1889 (2001). doi:10.1016/S0008-6223(00)00310-9
49. M.A. Montes-Morán, J.I. Paredes, A. Martínez-Alonso, J.M.D. Tascón, Surface characterization of PPTA fibers using inverse gas chromatography. Macromolecules **35**, 5085–5096 (2002). doi:10.1021/ma020069m
50. E. Papirer, E. Brendle, F. Ozil, H. Balard, Comparison of the surface properties of graphite, carbon black and fullerene samples, measured by inverse gas chromatography. Carbon **37**, 1265–1274 (1999). doi:10.1016/S0008-6223(98)00323-6
51. E. Díaz, S. Ordóñez, A. Vega, J. Coca, Characterization of Co, Fe and Mn-exchanged zeolites by inverse gas chromatography. J. Chromatogr. A **1049**, 161–169 (2004). doi:10.1016/j.chroma.2004.07.065
52. E. Díaz, S. Ordóñez, A. Vega, J. Coca, Catalytic combustion of hexane over transition metal modified zeolites NaX and CaA. Appl. Catal. B **56**, 313–322 (2005). doi:10.1016/j.apcatb.2004.09.016
53. E. Díaz, S. Ordóñez, A. Vega, A. Auroux, J. Coca, Benzylation of benzene over Fe-modified ZSM-5 zeolites: correlation between activity and adsorption properties. Appl. Catal. A **295**, 106–115 (2005). doi:10.1016/j.apcata.2005.07.059
54. N.A. Katsanos, N. Rakintzis, F. Roubani-Kalantzopoulou, E. Arvanitopoulou, A. Kalantzopoulos, Measurement of adsorption energies on heterogeneous surfaces by inverse gas chromatography. J. Chromatogr. A **845**, 103–111 (1999). doi:10.1016/S0021-9673(99)00262-9
55. N.A. Katsanos, Physicochemical measurements by the reversed-flow version of inverse gas chromatography. J. Chromatogr. A **969**, 3–8 (2002). doi:10.1016/S0021-9673(02)00992-5